ITER PHYSICS BASIS AND PHYSICS RULES

ITER Physics Expert Groups, ITER Physics Basis Editors,
ITER Joint Central Team, and ITER Home Teams*

presented by D. J. CAMPBELL
The NET Team, Max-Planck-Institut für Plasmaphysik, 85748 Garching, Germany

Abstract

In the course of the ITER EDA, an extensive collaboration amongst the major communities in the international magnetic confinement fusion programme has assembled a comprehensive description of the physics of tokamak plasmas. The *ITER Physics Basis* provides rules and methodologies for the extrapolation of plasma behaviour to the ITER scale and underpins both projections of plasma performance in, and the engineering design of, ITER. The major focus of the work has been the development of scalings and models for core, edge, and divertor plasmas in the ITER reference scenario, the ELMy H-mode. In addition, data relevant to ITER's ultimate goal of steady-state operation has been incorporated. Here the major elements of the ITER Physics Basis are summarized in terms of the understanding developed in the areas of plasma confinement, mhd stability and operational boundaries, the physics of edge and divertor plasmas, and energetic particle behaviour.

1. INTRODUCTION

A major benefit of the ITER EDA [1] has been the increased coherence of the world tokamak programme, which has focussed on establishing a reliable physics basis for the design of an ITER-scale experiment and for the prediction of its plasma performance [2]. There are three key aspects of this research. The first is the assembly of scaling databases derived from tokamak experiments, which provide broadly based scaling predictions for many aspects of ITER performance. The second consists of dedicated experiments designed to address specific physics questions, to validate theoretical concepts, and to develop operating scenarios in support of ITER. The third is the development of sophisticated numerical codes for modelling complex aspects of ITER behaviour and their validation in existing tokamak experiments. The experience gained in exploiting heating, current drive and diagnostic systems, and the physics understanding thereby developed, is an additional facet of these activities. This paper develops projection methodologies in the areas of plasma transport and confinement, mhd stability and operational limits, power and particle control, and energetic particle physics. Important conclusions which can be drawn from this activity are that a substantial basis now exists for the extrapolation of plasma behaviour to the ITER scale and that there is a common physics behaviour across many tokamak experiments which provides confidence in ITER performance predictions.

2. PLASMA CONFINEMENT

The ELMy H-mode is a reproducible and robust mode of tokamak operation with a demonstrated long-pulse capability. This is therefore the reference operating scenario for ITER ignited operation and the ITER Physics Basis naturally emphasizes observations and modelling in this regime. However, since steady-state operation remains an ultimate goal of the ITER programme, recent progress in 'advanced tokamak' scenarios, which are characterized in the main by low, or negative, central magnetic shear, has been incorporated in the Physics Basis. The results of ITER performance projections in this regime are reported in [3].

An empirical scaling database has been assembled for the prediction of the H-mode access conditions (eg [2]) using the working hypothesis that the plasma is sustained in H-mode by a minimum (conducted and convected) loss power flowing across the plasma separatrix. A

---

* Contributing authors to the ITER Physics Basis Document are listed in Reference [2].

significant recent advance is the confirmation in JET DT experiments that the dependence of the power threshold on the inverse of the plasma isotopic mass holds in DT and T plasmas [4], as illustrated in Fig. 1. The recommended log-linear scaling expression derived from the database is,

$$P_{thr} = C(R/a,\kappa,\alpha)M^{-1}B_T\bar{n}_{e,20}^{0.75}R^2(\bar{n}_{e,20}R^2)^{\alpha}, \quad (1)$$

in (MW, T, 10^{20}m^{-3}, AMU, m), with $-0.25\leq\alpha\leq0.25$, M the effective isotopic mass of the plasma fuel, and C a non-dimensional coefficient, with $C=(0.9\pm0.2)\times0.6^{\alpha}$. This predicts a midpoint loss power of 80MW for access to the H-mode in ITER at a density of $\langle n_e\rangle=5\times10^{19}$m^{-3}, with a factor of 2 uncertainty in either direction. Work is continuing to understand the sources of experimental scatter in the database so as to reduce this uncertainty and recent analysis is reported in [5].

Predictions of plasma transport, confinement, and fusion performance at the ITER scale are derived from an analysis which is founded on three complementary strands of physics R&D: (a) derivation of empirical global confinement scalings; (b) non-dimensionally similar transport and confinement studies; (c) development of one-dimensional transport modelling codes.

The first of these activities involves experimental data obtained from many tokamaks under a range of conditions. The extensive scope of the input data, the wide-ranging analysis which has been performed, and the understanding developed of the implications which the data selection and analysis techniques have for the extrapolation to ITER make this the recommended approach for characterizing confinement quality in ITER. Most recent improvements in the database (ITERH.DB3) have yielded a significantly better conditioned dataset [2, 5] in the sense that the database mean of each of the engineering parameters is closer to that of ITER and the ranges in the major parameters (R, n, I, P, B) are larger. The recommended scaling (IPB98y) for the thermal energy confinement time in the ITER reference scenario is,

$$\tau_{E,th}^{ELMy} = 0.0365I^{0.97}B^{0.08}P^{-0.63}n^{0.41}M^{0.20}R^{1.93}\varepsilon^{0.23}\kappa^{0.67}, \quad (2)$$

where the units are (s, MA, T, 10^{19}m^{-3}, AMU, m). Introducing the commonly used dimensionless variables ρ_*, β, and ν_*, this expression can be cast in the 'physics' form,

$$\tau_{E,th}^{ELMy} \propto \tau_B\rho_*^{-0.83}\beta^{-0.50}\nu_*^{-0.10}M^{0.97}q^{-2.52}\varepsilon^{-0.55}\kappa^{2.72}. \quad (3)$$

It is of significance that this scaling has an almost gyro-Bohm form.

Taking into account various forms of error analysis for the regression leading to equation (2), an interval estimate for the thermal confinement time at the ITER nominal operating point has been derived, $\tau_{E,th}^{ELMy} = (4.4,6.8)s$. This represents the 95% uncertainty level for a log-linear (ie power law) scaling analysis. When log-nonlinear models are included, a larger 95% interval estimate of $\tau_{E,th}^{ELMy} = (3.5,8.0)s$ results. However, the point estimates which emerge from all valid log-linear and log-nonlinear scalings derived to date lie within or above the smaller interval [2].

While the strength of the global scaling approach is that all physics factors influencing confinement are contained within the data, there are several weaknesses. Firstly, the various factors influencing confinement may scale differently from present devices to ITER, eg the contributions of core and edge pedestal to global confinement. Analysis of JET DT data indicates that core and edge confinement exhibit different dependences on the isotope mass, with the core confinement dependence lying close to that expected from pure gyro-Bohm scaling, $\tau_E^{core} \propto M^{-0.2}$ [4]. Secondly, the majority of data has been sampled away from operating boundaries, such as the density and β limits, and may not adequately reflect the confinement behaviour in the vicinity of these boundaries. Thirdly, there may be hidden parameters, such as the core Mach number (reflecting the influence of toroidal rotational shear), which are not included in the analysis. Several such issues are under investigation within the ITER framework.

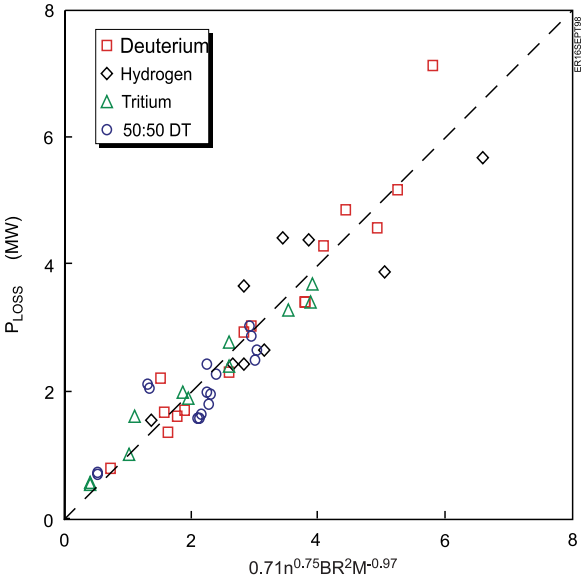

FIG. 1. H-mode power threshold data obtained from JET H, D, DT, and T plasmas, plotted against a regression fit to the data used to determine the isotopic mass scaling. Note that $P_{LOSS}=P_{IN}-dW/dt$.

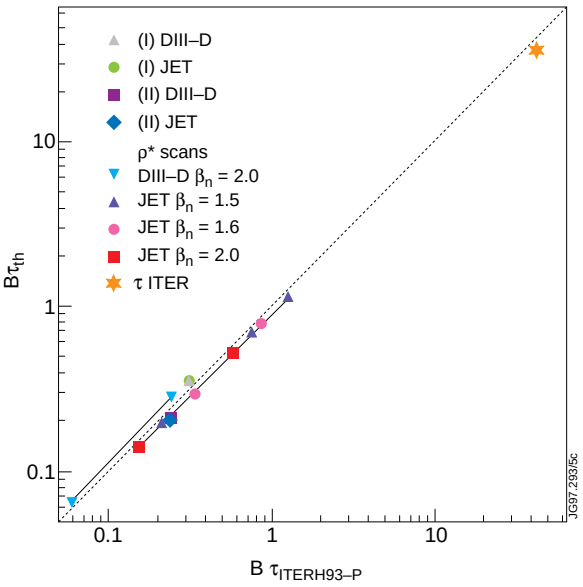

FIG. 2. Comparison of $B\tau_E$ measured in ρ_* scans in JET and DIII-D with the ITER93H-P scaling relation.

Kadomtsev's proposal that turbulence responsible for anomalous transport should depend on a small number of dimensionless parameters forms the basis of non-dimensional scaling analysis. This has given rise to the concept of ITER Demonstration Discharges, in which tokamaks have established plasmas in which β_N and ν_* are similar to those of ITER, allowing the dependence of transport and confinement on ρ_* to be addressed. Such experiments have shown that the dependence of ELMy H-mode confinement on ρ_*, the direction of largest extrapolation to ITER, scales in a gyro-Bohm fashion, in agreement with the global scaling expression. Figure 2 compares the results of non-dimensional scaling experiments in DIII-D and JET, one of several inter-device comparisons performed, and the ITER93H-P scaling, derived from an earlier version of the global database. Some discrepancies between the global and non-dimensional approaches remain and are the subject of further study. For example, while the latest global scaling has a $\beta^{-0.5}$ dependence, non-dimensional experiments find the confinement to be independent of β for $\beta_N<2$.

The third strand of activity involves the development of numerical codes for predicting the local transport properties of ITER plasmas from fundamental physics considerations. This has been greatly assisted by the code validation activity, using a database of experimental profiles from a range of tokamaks (eg [2]), which is essential for establishing the reliability of predictions for ITER. By using several figures of merit (eg the 'incremental' stored energy above that contained in the edge pedestal) tests have been performed on 11 models (see [2]). While each model performs well under specific circumstances, the present conclusion is that their predictive capability is not yet accurate enough to provide the principal basis for extrapolation to ITER.

3. MHD STABILITY AND OPERATIONAL LIMITS

MHD stability plays a defining role in determining the accessible parameter space, and thereby setting the limits of fusion performance. The major stability limits relate to the maximum plasma current, plasma density, and plasma pressure. Operating experience on many tokamaks underpins ITER's choice of operating at $q_{95}=3$ with $I_p=21$MA to achieve high confinement, by maximizing current, while avoiding the increasing susceptibility to instability as $q=2$ is approached. A quantitative analysis of disruption frequency on several tokamaks shows that ITER's goal of achieving an initial disruption frequency of 10% or less has been attained in existing devices, with no specific problems due to proximity to $q_{95}=3$ [6].

The β^2B^4 scaling of fusion power provides a substantial incentive to operate at the highest attainable β. The ideal β-limit, corresponding to $\beta_N=\beta/(I_p/aB))\sim3.5$, has been extensively validated in present devices, has also been confirmed for ITER by numerical analysis of reference equilibria using several mhd stability codes (see [2]), and affords ITER a considerable margin for operation at its nominal ignition point of $\beta_N=2.2$. However, the observation of neoclassical tearing modes at β_N values well below the ideal limit may pose a more significant constraint for ITER operation [2]. These modes develop as a result of an instability caused by a deficit of bootstrap current inside an island due to the flattening of the pressure profile across the island. Experimentally the most common modes have m,n=3,2, which generally leads to a 'soft' limit and a degradation of confinement, or m,n=2,1, which usually produces a major disruption.

Although a well developed theoretical explanation of the mode growth exists (eg [2]), the requirement for a 'seed' island, produced by other instabilities such as sawteeth, prevents the prediction of a precise limit in ITER. Figure 3 illustrates the β_N value at which neoclassical tearing modes were first observed in several tokamaks, plotted against the parameter $\nu_i/\varepsilon\omega_e^*$, which is important in determining the critical seed island size in the 'ion polarization current' model of the instability threshold. Although modes are observed at $\beta_N=2.2$ and below, the existence of long-pulse ITER Demonstration Discharges with the required values of β_N and ν_*, in experiments such as JET, provides support for the ITER reference scenario. In addition, the long growth time of the modes, 10-100s in ITER, could allow stabilization by localized ECCD and experiments to investigate this proposal are underway (eg [7]).

For ITER, two distinct density limiting processes are relevant. The ultimate limit for plasma density, generally observed in L-mode plasmas, is set by radiation and/or transport instabilities in the plasma edge and scrape-off layer, which trigger mhd instabilities leading to a major disruption. Of more relevance to the operating space for ignited operation is the common observation that it is difficult to maintain H-mode confinement while increasing the density with gas fuelling above the Greenwald scaling $\bar{n}_e(10^{20}m^{-3}) = I_p(MA)/\pi a^2(m)$. This limit is manifested as a gradual degradation of confinement which eventually results in a return to L-mode at densities somewhat lower than the L-mode limit (eg [2]). Pellet fuelling, particularly from the high field side of the plasma ('inside launch'), has enabled the density limit to be extended somewhat beyond the Greenwald value, though with some penalty in H-mode confinement quality, or a radiative collapse (see [2]). Operation in ITER requires a plasma density close to the Greenwald value and deep fuelling techniques such as inside pellet launch will therefore be required.

A possible explanation for the H-mode density limit has been developed in terms of an edge parameter operational diagram [8] (Fig. 4). It is proposed that H-mode confinement quality is influenced by the parameters of the pedestal and that in gas-fuelled discharges increasing the pedestal density at the expense of the pedestal temperature produces a transition from type I to type III ELMs and thence to L-mode. While the underlying physical processes have not yet been identified, this suggests that the density limit is (as in L-mode) an edge density limit.

The consequences of disruptions and vertical displacement events (VDEs) impose a significant design constraint on ITER and a characterization of disruptions in present devices has been developed which has allowed extrapolations of key processes to the ITER scale through the analysis of a multi-machine database (eg [2, 6]). Principal concerns include severe heat loads on the first wall and divertor targets, large electromechanical forces on the vessel structures, and potentially high currents of runaway electrons in the post-disruption plasma.

Thermal and poloidal field energies in ITER each amount to ~1GJ and the consequences of the disruption thermal and current quenches depend in large measure on the timescales of these events. The thermal quench is usually observed to occur in two stages, the first of which is most likely driven by resistive processes, while the second may involve mhd-driven convection and impurity radiation (see [2]). Analysis of the database indicates a timescale in ITER for the first phase of 20ms (uncertainty range: 6-60ms) and for the second phase of 1ms (uncertainty range: 0.3-3ms) [6]. While the spatial distribution of the energy deposited on the plasma facing surfaces is not well characterized, it is probable that localized energy deposition will reach $100MJm^{-2}$ at

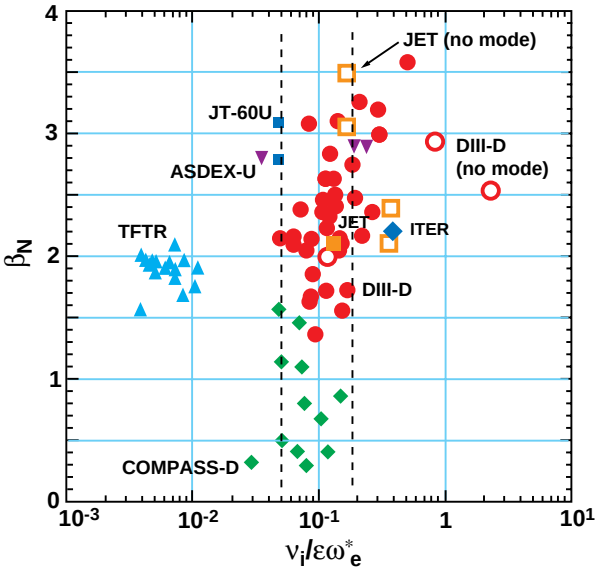

FIG. 3. Comparison of neoclassical mode onset data (closed points) from the ITER database with the predictions of the 'ion polarization current' threshold model (small threshold island width, $\nu_i/\varepsilon\omega^*_e < 0.3$; large threshold island width, $\nu_i/\varepsilon\omega^*_e > 0.3$). Open points are for no mode onset and the dashed vertical lines represent an experimental uncertainty.

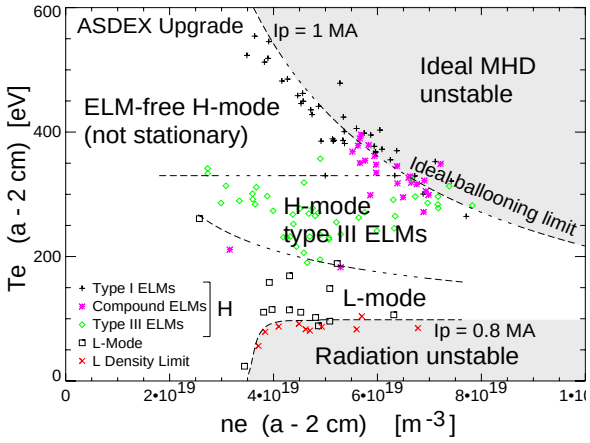

FIG. 4. ASDEX Upgrade edge pedestal diagram characterizing the confinement quality in terms of n_e and T_e measured 2cm inside the separatrix. Boundaries demarcating different confinement regimes are indicated.

the divertor target. Evaporation and melting of first wall materials can be expected at this level, but the occurrence of ablation shielding should mitigate the most severe effects (eg [2]).

Electromagnetic forces arise from: eddy current forces, due to the current quench, which increase with decreasing current quench times; and halo current induced forces, associated with VDEs, which are more severe for longer current quench times. Analysis indicates that the fastest current quench rate observed is consistent with a post-disruption plasma temperature of 3eV, which extrapolates to a minimum current quench time of 50ms in ITER [6]. The vessel forces due to VDEs depend on the magnitude of the halo current (for scaling purposes this is normalized to the plasma current, $I_{h,\max}/I_p$), and the degree of toroidal asymmetry, denoted toroidal peaking factor (TPF). Although the physics basis of halo currents is understood, the detailed processes determining the magnitude of these two quantities are not, and extrapolation to ITER again relies on database analysis. This has produced a design constraint for ITER of $(I_{h,\max}/I_p)\times TPF = 0.5$ for the 'typical case' and $(I_{h,\max}/I_p)\times TPF = 0.75$ for the 'worst case' (eg [2]). There is, in fact, an indication in the database that a favourable size scaling of $I_{h,\max}/I_p$ exists, and hence that the bound on maximum halo current fraction in ITER may eventually lie below 0.25.

Runaway electron currents can be generated by an avalanche process in the cold, highly impure plasma produced by disruptions. The runaway current level is predicted to reach as much as 15MA in ITER, with electron energies in the range 10-15MeV [2]. Interaction of such runaway electrons with the first wall could lead to localized surface damage, and suppression of runaway currents has become a central issue in the development of disruption mitigation and avoidance techniques. A promising development is that magnetic fluctuations associated with disruptions are found to suppress runaway electrons in JT-60U (eg [6]). Nevertheless, there is a requirement for a fast plasma shutdown system which can mitigate the most severe disruption effects (see [6]).

4. EDGE AND DIVERTOR PHYSICS

During the EDA, tokamak experiments have made major contributions to the development of a physics basis for the ITER power and particle exhaust concept by detailed investigations of

physics processes in the scrape-off layer and divertor and by incorporating ITER-relevant divertor geometries [2]. The central aim of these experiments has been to develop regimes in which divertor power dissipation due to (hydrogenic and impurity) radiation and volumetric charge exchange losses is enhanced, a high neutral pressure is maintained in the divertor to facilitate helium pumping, neutrals are effectively trapped in the divertor to prevent their outflow into the main chamber where they might influence edge conditions and confinement, and impurities are retained in the divertor to minimize plasma contamination.

In L-mode plasmas, it has been possible to achieve fully detached plasmas with hydrogenic gas puffing and many of the fundamental physics processes associated with detachment have been identified (see [2]). In particular, several theoretical expectations, for example the role of recombination losses in power dissipation and the low divertor temperatures (1-2eV) required for detachment, have been confirmed experimentally. In contrast, in H-mode plasmas, divertor detachment can only be sustained in impurity seeded discharges, in which low levels of impurity gases such as argon, neon, or nitrogen are combined with hydrogenic gas puffing to enhance radiation levels and establish plasma detachment (see [2]). Virtually all divertor tokamaks, and some limiter devices, have established such regimes, but at some penalty in the global energy confinement (eg [9]). Although the level of impurity contamination in present devices is unacceptably high, the scaling study performed in [9] indicates that the parametric dependence of the impurity concentration scales in an acceptable way to ITER. This is supported by detailed modelling calculations of the ITER divertor (see [2]).

The introduction of ITER-like geometries in a number of devices, involving vertical divertor targets with a closely baffled divertor volume, has produced several of the anticipated effects (eg [10]). For example, higher neutral densities and hence higher neutral compression factors (of order 100) are observed, higher power losses occur due to the increased volumetric recombination and, as a result, plasma detachment from the divertor is initiated at lower density and the target power loading is reduced. This has also had a significant beneficial impact on helium pumping capability. However, thus far divertor geometry has neither influenced the core plasma impurity levels, nor had a discernible impact on H-mode core plasma performance.

Experiments in DIII-D have demonstrated that in ELMy H-modes helium can be exhausted at a rate which satisfies the constraint $\tau^*_{He}/\tau_E \leq 15$ (see [2]) and that the exhaust rate is determined by the achievable pumping speed, rather than by core transport processes, a key result for ITER. Moreover, studies in ASDEX Upgrade and in the W-shaped divertor in JT-60U have shown that $\tau^*_{He}/\tau_E \sim 5-10$ can be attained in ELMy H-modes (eg [10]), supporting modelling predictions that the helium concentration can be maintained below 10% in an ignited plasma.

The complexity of processes in the SOL and divertor, combined with the fact that the relationships between physics scale-lengths and divertor size in ITER differ significantly from those in current devices, necessitates the use of sophisticated two-dimensional SOL and divertor modelling codes for the prediction of divertor performance in ITER. Results flowing from the experiments have provided validation of physics concepts incorporated in such codes (see [2]) and many of the experimentally observed phenomena can be reproduced. However, perpendicular transport in the SOL, which is still poorly understood, must be described by empirical scalings from existing experiments. A database characterizing SOL parameters has been assembled and the current status of the scaling analysis is discussed in [11]. In addition, the predictions for divertor performance in ITER derived from such codes are reviewed in [12] and indicate that a substantial operating window with acceptable power loads and helium exhaust rates exists.

5. ENERGETIC PARTICLE BEHAVIOUR

The essential issues in energetic particle physics are that the α-particles (and other fast ion species) must slow down classically and not suffer anomalous losses due to mhd instabilities or TF ripple. The first requirement has been convincingly demonstrated in tokamak experiments, where energetic particles produced by auxiliary heating systems do slow down and transfer their energy to the thermal plasma at the predicted rate (eg [2, 13]). Additional evidence has come from DT experiments in TFTR [14] and JET [15], where electron heating by α-particles was as expected.

The influence of TF ripple on energetic particle losses has been studied experimentally in several devices using fast particle populations produced by NBI and ICRF (see [2]), as well as fusion-produced α-particles in TFTR (eg [16]). These experiments have tested and validated numerical codes which incorporate the various TF ripple loss mechanisms identified theoretically. The good agreement between experimental observations and code computations gives confidence in the predictions for ITER that α-particle losses will be acceptable in both the reference ignited and proposed steady-state scenarios (the major consideration is to avoid damage to the first wall) .

Energetic particles influence the stability properties of mhd instabilities, contributing both stabilizing and destabilizing effects. For example, sawtooth stabilization has been studied both experimentally and theoretically, leading to the development of a model for the sawtooth instability in ITER (eg [2]) which predicts that sawteeth could be stabilized transiently for up to 100s by α-particles. The residual uncertainties in the theory of the m=1 instability give rise to significant uncertainties in this prediction, but the result is indicative of the way in which the α-population might change the mhd behaviour of an ignited plasma. Additional instabilities which might interact with α-particles and other energetic particle populations include fishbones, kinetic ballooning modes, localized interchange modes, neoclassical tearing modes, and ELMs (see [2]).

Attention in this area has focussed on the role of α-particles in exciting Alfvén eigenmodes (AEs), since the α-particle energy is well above that (~1.3MeV in ITER) associated with the Alfvén velocity and the α-population can resonantly destabilize these modes via the free energy available in the α-pressure gradient (see [2]). The specific concern arising from this interaction is that AEs could eject a significant fraction of the α-population from the plasma, causing damage to the first wall. The modes have been studied in both tokamak and stellarator experiments using, for the most part, the fast ion populations produced by NBI and ICRF heating (eg [13]).

Validation of numerical codes employed in calculating Alfvén eigenmode stability is a central aspect of these studies. Broadly speaking, it is found that the predictions of mode frequencies and structures are in good agreement with experimental observations. Stability thresholds, which are more problematic due to the competition between α-particle drive and damping arising from several dissipative mechanisms associated with the background plasma, are found to be in reasonable agreement (see [2]). On the basis of such detailed comparisons, the numerical codes have been used to predict Alfvén eigenmode stability in ITER. It seems likely that the major source of concern will involve the nonlinear interaction of the α-population with modes having higher toroidal mode numbers (n>10), for which further theoretical developments are required. The implications of these calculations for ITER are discussed in detail in [17].

Although the volume averaged α-particle β in ITER, $<\beta_\alpha>$, exceeds that in existing DT experiments (0.2% versus 0.12% in JET), it is lower than that of fast particle populations produced by auxiliary heating systems in current devices (up to 0.5% in ICRH experiments) [2]. Moreover, the dimensionless fast ion pressure gradient, $R\nabla\beta_f$, which drives collective fast ion instabilities, is also lower (0.06) than in some present devices (up to 0.1). While plasma dimensionless parameters in current experiments do not entirely match those in ITER, the extensive experimental and numerical studies performed have encompassed the range of fast particle parameters expected in ITER and provide an acceptable basis for the extrapolation of confinement and mhd stability aspects of α-particle behaviour to ITER conditions. Analysis indicates that confinement of α-particles will be sufficiently good to allow efficient α-particle heating and that anomalous losses will be within design constraints on first wall power loading.

6. DISCUSSION AND CONCLUSIONS

This paper has briefly reviewed several key aspects of the ITER Physics Basis, identifying the major issues which define the performance capability of a reactor scale experiment, outlining key elements of the rules and models which have been developed to extrapolate plasma performance to ITER, and summarizing remaining areas of uncertainty. It has not been possible to touch on the extensive contributions which have also been made in the fields relating to plasma control, plasma diagnostics, and plasma heating and current drive systems, which have established

confidence in ITER's capability to operate as foreseen. To quote a single example, the recent JET DT experiments have studied and validated ICRF scenarios proposed for ITER [18].

The experimental observations and analysis assembled in the ITER Physics Basis [2] provides a guiding methodology for extrapolating plasma performance to the ITER scale and underpins the predictions that ITER will achieve its goal of long-pulse controlled ignition [1]. On the basis of the recommended scalings for the H-mode power threshold and ELMy H-mode energy confinement outlined in Section 2, it is predicted that ITER has a significant window for ignited operation, with some margin for confinement degradation [1, 2]. The major uncertainties are associated with the H-mode power threshold and confinement behaviour close to the operational boundaries discussed in Section 3. In the course of the EDA there have been considerable advances in the understanding of the physics of these boundaries as they apply to ITER. While there are remaining uncertainties in the predictions of the precise β and density limits for ITER, experimental techniques under development, such as ECCD control of neoclassical tearing modes and inside pellet launch for operation at high density, will contribute to ITER's operational flexibility in these areas. These techniques, together with the ability, for example, to operate at currents above 21MA, will strengthen ITER's performance margins. Overall, the projections for plasma performance in the ITER ELMy H-mode reference scenario can be considered to be founded on the most systematic analysis of evidence available from existing experiments and these projections give confidence that ITER will meet its goal of long pulse ignited operation.

ACKNOWLEDGEMENTS

The ITER Physics Basis has been assembled as the result of an extensive collaboration involving the ITER Physics Expert Groups and a large number of additional contributors from the international fusion community who have voluntarily pooled their knowledge and expertise to provide the overview of tokamak physics which has been so briefly discussed in this paper.

This report is an account of work undertaken within the framework of the ITER EDA Agreement. The views and opinions expressed herein do not necessarily reflect those of the Parties to the ITER EDA Agreement, the IAEA or any agency thereof. Dissemination of the information in these papers is governed by the applicable terms of the ITER EDA Agreement.

References

[1] Technical Basis for the Final Design Report, Cost Review and Safety Analysis, ITER EDA Documentation Series, (to be published) IAEA, Vienna (1998).
[2] ITER PHYSICS EXPERT GROUPS et al., "The ITER Physics Basis", Nucl. Fusion (to be published).
[3] BOUCHER, D., et al., "Assessment and Modeling of Inductive and Non-Inductive Scenarios for ITER", these Proceedings.
[4] THE JET TEAM (presented by K. THOMSEN), "H-mode Power Threshold and Confinement in JET H, D, D-T and T Plasmas", Plasma Phys. Control. Fusion (to be published).
[5] THOMSEN, K., et al., "Latest Results from the ITER H-Mode Confinement and Threshold Data Bases", these Proceedings.
[6] YOSHINO, R., et al., "Characterization of Disruption Phenomenology in ITER", these Proceedings.
[7] ZOHM, H., et al., Plasma Phys. Control. Fusion **39** (1997) B237-B246.
[8] KAUFMANN, M., et al., in Fusion Energy 1996 (Proc. 16th Int. Conf., Montréal, 1996), Vol. 1, IAEA, Vienna (1997) 79-94.
[9] MATTHEWS, G. F., et al., J. Nucl. Mater. **241-243** (1997) 450-455.
[10] BOSCH, H. S., et al., "Effect of Divertor Geometry on Boundary and Core Plasma Performance in ASDEX Upgrade and JET", Plasma Phys. Control. Fusion (to be published).
[11] SHIMADA, M., et al., "Edge Database Analysis for Extrapolation to ITER", these Proceedings.
[12] KUKUSHKIN, A. S., et al., "2D Modelling and Assessment of Divertor Performance for ITER", these Proceedings.
[13] HEIDBRINK, W. W., SADLER, G. J., Nucl. Fusion **34** (1994) 535-615.
[14] TAYLOR, G., et al., Phys. Rev. Lett. **76** (1996) 2722-2725.
[15] THOMAS, P. R., et al., Phys. Rev. Lett. **80** (1998) 5548-5551.
[16] HAWRYLUK, R. J., et al., Phys. Plasmas **5** (1998) 1577-1589.
[17] PUTVINSKI, S., et al., "Energetic Particles and Runaway Electrons in ITER", these Proceedings.
[18] START, D. F. H., et al., Phys. Rev. Lett. **80** (1998) 4681-4684.